

Modeling, Stability and Numerical Simulation of Doxorubicin Transport and Uptake in Tumors.

Daniela Cortes¹ Giuseppe Romanazzi²
IMECC, Campinas, SP

Abstract. This work analyzes the transport and effect of the chemotherapy drug doxorubicin in tumors. Specifically, we model the diffusion-convection process of doxorubicin delivered by bolus injection across the tumor and interstitium by a system of partial differential equations. We present a stability analysis of the system solution and implement a finite difference method to approximate it.

Keywords. Difusion-Convection, Interstitium, Stability

1 Introduction

For modeling the transport and uptake of anticancer drugs in tumors, we consider the free (C_f), bound to proteins (C_b), and intracellular (C_i) concentrations of doxorubicin and the density of tumor cells (D_c). We considered factors as cell degradation, proliferation, and doxorubicin binding to proteins are used in the model; see [4, 6, 7].

After describing the partial differential equations model in Section 2, we introduce in Section 3 a second-order finite difference method applied to the model, see [2]. In Section 4 we then illustrate the numerical results obtained by implementing the numerical method using the © Matlab software [5]. In Section 5 we analyze and provide results for the stability of the partial differential equations model system solution. Finally we present the final considerations of this work in Section 6.

2 Modeling the Drug Transport and Uptake

Our model is based on the work [7], which considers the following assumptions:

- The tumor is spherical, with a radius of R_o ; the tumor's interior is in the center and occupies the volume of a sphere of radius R_i .
- Concentrations of doxorubicin within the tumor and tumor density are time-dependent and vary with distance r from the center of the sphere.
- Two boundaries exist an inner boundary that separates tumor tissue from normal tissue and an outer boundary of normal tissue.
- On the internal boundary, we apply continuity conditions for free concentration and fluid flux.
- On the outer boundary, we assume a zero flux of drug concentration.

¹danielac@ime.unicamp.br

²groman@unicamp.br

- The diffusion coefficients are constants in time and space.

The novelty with respect to the model [7] is that we suppose that the velocity is constant in time see [1], and we add a degradation term in the tumor cell density equation.

Under the aforementioned assumptions, the transport of free doxorubicin within the tumor is described by the following initial boundary problem

$$\left\{ \begin{array}{l} \frac{\partial C_f}{\partial t}(r, t) + \operatorname{div}(C_f(r, t)v(r)) = D_{ft}\Delta C_f(r, t) + F_1(r, t) \quad \text{in } B(R_i), \quad t \in (0, T], \\ \frac{\partial C_f}{\partial t}(r, t) + \operatorname{div}(C_f(r, t)v(r)) = D_{fn}\Delta C_f(r, t) + F_2(r, t) \quad \text{in } B(R_o \setminus R_i), \quad t \in (0, T], \\ D_{ft} \frac{\partial C_f}{\partial r}(R_i, t) = D_{fn} \frac{\partial C_f}{\partial r}(R_i, t), \quad t \in (0, T], \\ v(R_o)C_f(R_o, t) - D_{fn} \frac{\partial C_f}{\partial r}(R_o, t) = 0, \quad t \in (0, T], \\ C_f(r, 0) = C_{f0}, \end{array} \right. \quad (1)$$

where $B(R_i) = \{x \in \mathbb{R}^3, 0 < \|x\| < R_i\}$, $B(R_o \setminus R_i) = \{x \in \mathbb{R}^3, R_i < \|x\| < R_o\}$ and with F_1, F_2 given below

$$\begin{aligned} F_1 &= V_{max} \left(\frac{C_i(r, t)}{C_i(r, t) + k_i} - \frac{C_f(r, t)}{C_f(r, t) + k_e\varphi} \right) D_c(r, t), \\ F_2 &= k_v \frac{S}{V} (p_v - p_i(r) - \sigma_T(\pi_v - \pi_i)) (1 - \sigma) C_v(t) + P \frac{S}{V} (C_v(t) - C_f(r, t)) \frac{P_{ev}}{e^{P_{ev}} - 1} \\ &\quad - k_l \frac{S_l}{V} (p_i(r) - p_l) C_f(r, t) + k_d C_b(r, t) - k_a C_f(r, t). \end{aligned} \quad (2)$$

In F_1 there are the following parameters: V_{max} the maximum rate of trans-membrane transport, k_e and k_i are obtained from experimental data [7], φ is the volume fraction of extracellular space. In F_2 we have: C_v being the concentration of doxorubicin in blood plasma, P_{ev} is the trans-capillary Peclet number, k_v is the hydraulic conductivity of the microvascular wall, p_v and p_i are the vascular and interstitial fluid pressure respectively, σ_T represents the average osmotic reflection coefficient for plasma protein, π_v is the osmotic pressure of the plasma, and π_i is that of the interstitial fluid, P is the vascular permeability, k_l is the hydraulic conductivity of the lymphatic wall, S_l/V is the surface area of lymphatic vessels per unit volume of tissue, and p_l is the intra-lymphatic pressure, S/V is the surface area of blood vessels per unit volume of tissue, k_a and k_d are the doxorubicin-protein binding and dissociation rate, respectively.

Within the region $B(R_o \setminus R_i)$, certain proteins have the ability to bind with C_f , resulting in the transformation of C_f to C_b . This phenomenon can be mathematically represented through the following system of equations for C_b , along with its respective boundary initial conditions

$$\left\{ \begin{array}{l} \frac{\partial C_b}{\partial t}(r, t) + \operatorname{div}(v(r)C_b(r, t)) = D_b\Delta C_b(r, t) + k_a C_f - k_d C_b, \quad \text{in } B(R_o \setminus R_i), \quad t \in (0, T], \\ v(R_i)C_b(R_i, t) - D_b \frac{\partial C_b}{\partial r}(R_i, t) = 0, \quad t \in (0, T], \\ v(R_o)C_b(R_o, t) - D_b \frac{\partial C_b}{\partial r}(R_o, t) = 0, \quad t \in (0, T], \\ C_b(r, 0) = C_{b0}. \end{array} \right. \quad (3)$$

Over time, a quantity of free doxorubicin enters the interior of the tumor by crossing its inner boundary. This doxorubicin concentration intracellular C_i , can be modeled by the following ordinary differential initial value problem

$$\begin{cases} \frac{\partial C_i}{\partial t}(r, t) = V_{max} \left(\frac{C_f(r,t)}{C_f(r,t)+k_e\varphi} - \frac{C_i(r,t)}{C_i(r,t)+k_i} \right), & \text{in } B(R_i), \quad t \in (0, T], \\ C_i(r_i, 0) = 0. \end{cases} \quad (4)$$

We model the interaction between intracellular concentration and cell density D_c by

$$\begin{cases} \frac{\partial D_c}{\partial t}(r, t) = \left(k_p - \frac{f_{max}C_i(r,t)}{C_i(r,t)+EC_{50}} \right) D_c(r, t) - k_m D_c^2(r, t), & \text{in } B(R_i), \quad t \in (0, T], \\ D_c(r_i, 0) = D_{c0}, \end{cases} \quad (5)$$

where f_{max} is the cell-kill rate constant, and EC_{50} is the drug concentration producing 50% of f_{max} . And the constants k_p and k_m are the cell proliferation rate constant and physiologic degradation rate, respectively.

3 Finite Differential Method

In this section, we describe the numerical method used to approximate the solution of (1), (3), (4), and (5). We discretize the spatial domain $[0, R_o]$ by the non-uniform grid R given by $R = \{r_j \in \mathbb{R}, j = 0, \dots, N_1 + N_2\}$ where $r_j - r_{j-1} = h_j$, $r_0 = 0, r_{N_1} = R_i, r_{N_1+N_2} = R_o$, the time domain $[0, T]$ is discretized by $\{t_n, n = 0, \dots, M\}$ with $t_0 = 0, t_M = T$ and constant step-size Δt .

The numerical method consists in finding $C_f^n, C_b^n, C_i^n, D_c^n$ satisfying (1), (3), (4), and (5). These equations are:

$$\begin{aligned} D_{-t}C_{f,j}^n &= \frac{D_{ft}}{r_j^2} D_h^* \left(M_h(r_j^2) D_h C_{f,j}^n \right) - \frac{1}{r_j^2} D_{cen} \left(r_j^2 v_j C_{f,j}^n \right) + F_{1,j}^n, \quad j = 0, \dots, N_1 - 1, \\ D_{-t}C_{f,j}^n &= \frac{D_{fn}}{r_j^2} D_h^* \left(M_h(r_j^2) D_h C_{f,j}^n \right) - \frac{1}{r_j^2} D_{cen} \left(r_j^2 v_j C_{f,j}^n \right) + F_{2,j}^n, \quad j = N_1 + 1, \dots, N_1 + N_2 - 1, \\ D_{-t}C_{b,j}^n &= \frac{D_b}{r_j^2} D_h^* \left(M_h(r_j^2) D_h C_{b,j}^n \right) - \frac{1}{r_j^2} D_{cen} \left(r_j^2 v_j C_{b,j}^n \right) + k_a C_{f,j}^n - k_d C_{b,j}^n, \quad j = N_1 + 1, \dots, N_1 + N_2 - 1, \\ D_{-t}C_{i,j}^n &= V_{max} \left(\frac{C_{f,j}^n}{C_{f,j}^n + k_e\varphi} - \frac{C_{i,j}^{n-1}}{C_{i,j}^{n-1} + k_i} \right), \quad j = 0, \dots, N_1 - 1, \\ D_{-t}D_{c,j}^n &= \left(k_p - \frac{f_{max}C_{i,j}^n}{C_{i,j}^n + EC_{50}} \right) D_{c,j}^{n-1} - k_m (D_{c,j}^{n-1})^2, \quad j = 0, \dots, N_1 - 1, \end{aligned} \quad (6)$$

In which C_f^n represents the set of approximate solutions of $C_f(r_j, t_n)$, in a similar way we have for C_b^n, C_i^n , and D_c^n . Additionally, let's $M_h(r_j) = \frac{r_j+r_{j-1}}{2}$ be the average operator. We specify in what follows the discretization of the boundary conditions given in (1) and (3).

At $r = R_o$ we consider

$$v_{R_o} C_{f,R_o}^{n+1} - D_{fn} D_{cen} C_{f,R_o}^{n+1} = 0, \quad v_{R_o} C_{b,R_o}^{n+1} - D_b D_{cen} C_{b,R_o}^{n+1} = 0. \quad (7)$$

At $r = R_i$ we have

$$-D_{ft}D_{cen}C_{f,R_i}^{n+1} + D_{fn}D_{cen}C_{f,R_i}^{n+1} = 0, \quad v_{R_i}C_{b,R_i}^{n+1} - D_bD_{cen}C_{b,R_i}^{n+1} = 0. \quad (8)$$

At $r = 0$ we consider

$$D_{cen}C_{f,r}^{n+1} = 0. \quad (9)$$

Finally, with the initial conditions

$$C_{f,j}^0 = 0, \quad C_{b,j}^0 = 0, \quad C_{i,j}^0 = 0, \quad D_{c,j}^0 = D_{co}, \quad j = 0, \dots, N_1 + N_2, \quad (10)$$

we complete the finite-difference system (6).

The discrete operators used in (6) are given by

$$\begin{aligned} D_{-t}v(r^n) &= \frac{v(r^n) - v(r^{n-1})}{\Delta t}, & D_{cen}v(r_j) &= \frac{v(r_{j+1}) - v(r_{j-1}))}{h_j + h_{j+1}}, \\ D_hv(r_{j+1/2}) &= \frac{v(r_{j+1}) - v(r_j)}{h_{j+1}}, & D_h^*v(r_j) &= \frac{v(r_{j+1/2}) - v(r_{j-1/2}))}{h_{j+1/2}}, \end{aligned} \quad (11)$$

where $h_{j+1/2} = \frac{h_j + h_{j+1}}{2}$.

The numerical method in (6) is implicit-explicit discretized in time and space using discrete operators of the second order in space and the first order in time. These discretizations are similar to those used in [2]; since the discrete operators used in space are of order 2. We will prove in future works that this numerical method converges with order 2, using a proof similar to that used in [2, 3].

4 Numerical results

We present several numerical simulations of model (1), (3), (4), and (5) by implementing the numerical method (6)–(10) using the © Matlab Software. A time step of $\Delta t = 10^{-5}$ and a constant step-size of $h_j = 3.7 \cdot 10^{-3}$ in the interval $(0, R_i)$, and another constant $h_j = 6.2 \cdot 10^{-3}$ in the interval (R_i, R_o) are used.

The figures below illustrate the values of C_f , C_b , C_i , and D_c obtained at various times T (in minutes) and in all domain $[0, R_o]$.

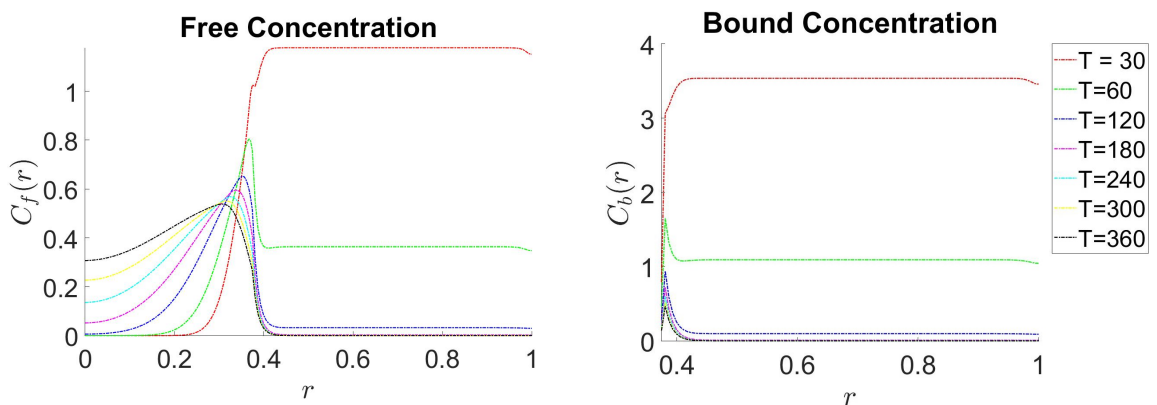


Figure 1: Free and Bound Doxorubicin Concentration in $\frac{\mu g}{ml}$ in spatial domain.

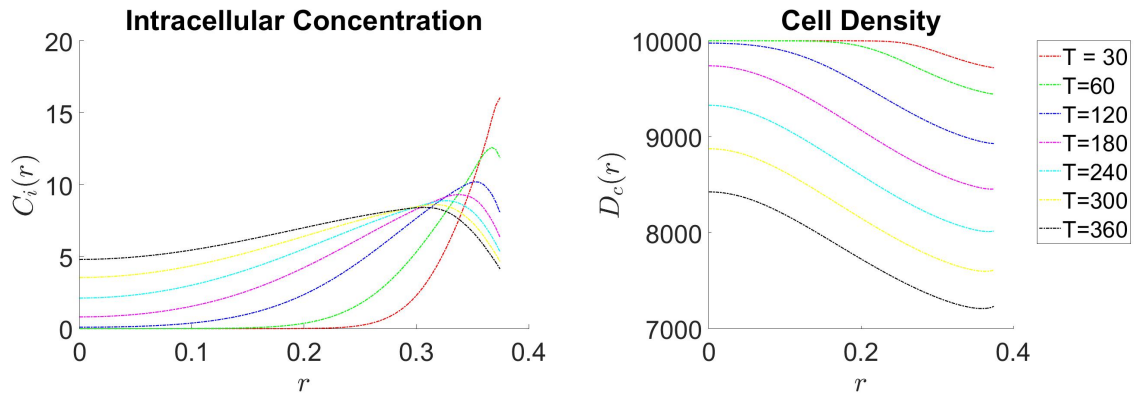


Figure 2: Intracellular Doxorubicin Concentration in $\frac{ng}{10^5 cells}$ and Cell Density in $\frac{10^5 cells}{ml}$ in tumor domain.

Note that in Figures 1 and 2, the radial axis is normalized. The problem parameters and constants are the same as those used in [7], with an applied bolus injection dose of $85600 \mu g/m^2$ representing the adequate dose for a $70kg$ patient. From Figure 1 we note that the free concentration C_f behaves as expected in the tumor tissue ($r \in [0, 0.5]$) during the first 6 hours of drug injection. In fact, it increases its values up to a value of around $0.3 \mu g/ml$ in the middle of the tumor corresponding to around a value of $5.5 \cdot 10^{-4} mol/m^3$ a value that is in the range of that expected in the numerical results provided in [7] when a drug infusion is applied. Instead in the normal tissue ($r \in [0.5, 1]$) the free concentration rapidly decrease along the time reaching already after one hour of drug injection a value of $0.3 \mu g/ml$. This is due to the much higher permeability of the tumor tissue respect the normal tissue. We observed in general that that the free concentration is higher respect that obtained numerically in [7] especially in the normal tissue where a second-order upwind scheme coupled with Backward Euler in time has been used to discretize the drug equations. This difference can be due to the pressure-velocity equation in the normal tissue that is not solved in our current work. Despite this discrepancy in the absolute values of free concentration in normal tissue, we have as in [7] that the bound concentration is almost three times the free concentration, see Figure 1. In Figure 2 we observe that intracellular concentration increases rapidly in the last hour reaching a value of almost $5 \frac{ng}{10^5 cells}$ as that expected in [7] where a maximum value of $4.5 \frac{ng}{10^5 cells}$ is reached for drug infusion. Also we observe a decreasing in time of the tumor density D_c of around 15% as that expected in [7] after six hours of bolus injection.

5 Estimate of the solutions C_f , C_b , C_i , and D_c

This section showcases the results derived from the solutions' stability analysis and theoretical estimations.

Theorem 5.1. *Let $E(t)$ be defined by*

$$E(t) := \|C_f(t)\|_{L^2(\Omega)}^2 + \|C_b(t)\|_{L^2(R_o \setminus R_i)}^2 + \|D_c(t)\|_{L^2(R_i)}^2, \quad (12)$$

and let C_f, C_b, D_c solutions of (1), (3) and (5) respectively, then there exists positive constant σ such that

$$E(t) + \int_0^t \left(\|\nabla C_f(t)\|_{L^2(\Omega) \times L^2(\Omega)}^2 + \|\nabla C_b(t)\|_{L^2(R_o \setminus R_i) \times L^2(R_o \setminus R_i)}^2 \right) d\mu \leq K e^{\sigma t}, \quad t \in [0, T], \quad (13)$$

where, $K = \|C_f(0)\|_{L^2(\Omega)}^2 + \|C_b(0)\|_{L^2(R_o \setminus R_i)}^2 + \|C_v(0)\|_{L^2(R_o \setminus R_i)}^2 + \|D_c(0)\|_{L^2(R_i)}^2$.

Theorem 5.2. *Let C_i solution of (4), we have the next estimate*

$$\|C_i(t)\|_{L^2(R_i)}^2 \leq \left(\|C_i(0)\|_{L^2(R_i)}^2 + V_{max}^2 |\Omega| \right) e^{2t} - V_{max}^2 |\Omega|, \quad (14)$$

where, $|\Omega|$ denotes the total volume measure.

Corollary 5.1. *We consider the system (1) without the source terms, and (3). Theorem 5.1 guarantees its stability. That is, let \bar{C}_ℓ and \hat{C}_ℓ with $\ell \in \{f, b\}$ be solutions of (1) and (3) with their respective initial conditions $\bar{C}_\ell(0) = \bar{C}_{\ell 0}$ and $\hat{C}_\ell(0) = \hat{C}_{\ell 0}$ and we define $w_{C_\ell}(t) = \bar{C}_\ell(t) - \hat{C}_\ell(t)$. Then, there exists positive constant α such that*

$$\|w_{C_\ell}(t)\|_{L^2(\Omega)}^2 + \int_0^t \|\nabla w_{C_\ell}(\mu)\|_{L^2(\Omega) \times L^2(\Omega)}^2 d\mu \leq \|w_{C_\ell}(0)\|_{L^2(\Omega)}^2 e^{\alpha T}. \quad (15)$$

Theorem 5.3. *Let \bar{C}_i and \hat{C}_i solutions of (4) with their respective initial conditions $\bar{C}_i(0) = \bar{C}_{i0}$ and $\hat{C}_i(0) = \hat{C}_{i0}$. We define $w_{C_i}(t) = \bar{C}_i(t) - \hat{C}_i(t)$. Then there exists positive constant β such that*

$$\|w_{C_i}(t)\|_{L^2(R_i)}^2 \leq \|w_{C_i}(0)\|_{L^2(R_i)}^2 e^{\beta T}. \quad (16)$$

Theorem 5.4. *Let \bar{D}_c and \hat{D}_c solutions of (5) bounded below by a constant M with their respective initial conditions $\bar{D}_c(0) = \bar{D}_0$ and $\hat{D}_c(0) = \hat{D}_0$, for $t \in [0, T]$.*

We define $w_{D_c}(t) = \bar{D}_c(t) - \hat{D}_c(t)$. Then there exists positive constant γ such that

$$\|w_{D_c}(t)\|_{L^2(R_i)}^2 \leq \|w_{D_c}(0)\|_{L^2(R_i)}^2 e^{\gamma T}. \quad (17)$$

The previous theorems will not be proved here.

6 Conclusions

Based on the relation between the free concentration (C_f) and the intracellular concentration (C_i) shown in Figuras 1 and 2, it is observed that for larger times, they will reach equilibrium. This is because the diffusive phenomenon becomes dominant, and it causes the density of the tumor cells (D_c) to stop growing.

References

- [1] L. T. Baxter and R. K. Jain. "Transport of fluid and macromolecules in tumors. I. Role of interstitial pressure and convection". In: **Microvascular Research** 1 (1989), pp. 77–104. DOI: 10.1016/0026-2862(89)90074-5.
- [2] J. S. Borges et al. "Drug release from viscoelastic polymeric matrices-a stable and supraconvergent FDM". In: **Computers & Mathematics with Applications** (2021), pp. 257–269. DOI: 10.1016/j.camwa.2021.08.007.

- [3] G. C. M Campos, J.A. Ferreira, and G. Romanazzi. “Density-pressure IBVP: Numerical analysis, simulation and cell dynamics in a colonic crypt”. In: **Applied Mathematics and Computation** 424.127037 (2022).
- [4] S. Eikenberry. “A tumor cord model for doxorubicin delivery and dose optimization in solid tumors”. In: **Theoretical Biology and Medical Modelling** 1 (2009), pp. 1–20. DOI: 10.1186/1742-4682-6-16.
- [5] The MathWorks Inc. **MATLAB version: 9.13.0 (R2022b)**. Natick, Massachusetts, United States, 2022. URL: <https://www.mathworks.com>.
- [6] A. W. El-Kareh and T. W. Secomb. “A mathematical model for comparison of bolus injection, continuous infusion, and liposomal delivery of doxorubicin to tumor cells”. In: **Neoplasia** 4 (2000), pp. 325–338. DOI: 10.1038/sj.neo.7900096.
- [7] W. Zhan, W. Gedroyc, and X. Yun Xu. “Mathematical modelling of drug transport and uptake in a realistic model of solid tumour”. In: **Protein and Peptide Letters** 11 (2014), pp. 1146–1156. DOI: 10.2174/0929866521666140807115629.